Computational Fluid Dynamics Prediction of the Reacting Flowfield Inside a Subscale Scramjet Combustor

Tawit Chitsomboon*
ViGYAN, Inc., Hampton, Virginia 23665
and
G. Burton Northamt†
NASA Langley Research Center, Hampton, Virginia 23665

A three-dimensional, Reynolds-averaged Navier-Stokes computational fluid dynamics (CFD) code has been used to calculate the reacting flowfield inside a hydrogen-fueled subscale scramjet combustor. Pilot fuel was injected transversely upstream of the combustor, and the primary fuel was injected transversely downstream of a backward facing step. A finite-rate combustion model with two-step kinetics was used. The CFD code used the explicit MacCormack algorithm with point implicit treatment of the chemistry source terms. Turbulent mixing of the jets with the airstream was simulated by a simple mixing length scheme, whereas near-wall turbulence was accounted for by the Baldwin-Lomax model. Computed results were compared with experimental wall pressure measurements.

Nomenclature

f_i = mass fraction of the ith chemical species
k = adjustable constant in the turbulence model
l = mixing length for the turbulence model
M = Mach number
n = direction normal to a solid wall
p = pressure
T = temperature
μ_t = turbulence viscosity
ϕ_1 = equivalence ratio of pilot fuel
ϕ_2 = equivalence ratio of primary fuel
ρ = density
ω = vorticity

Introduction

IT is generally acknowledged that computational fluid dynamics (CFD) will have to play an important role for a timely success of the National Aerospace Plane (NASP) program. Before CFD codes can be used routinely with confidence, they need to be validated with realistic and accurate experimental data. The objective of this study was to validate an existing three-dimensional CFD code with the experimental data of the subscale scramjet combustor test conducted at the Hypersonic Propulsion Branch, NASA Langley Research Center. The results in this paper give the status of our progress in validating CFD codes and studying scale effects of scramjet models.

The flowfield inside a scramjet combustor is rather complex, mainly as a result of the presence of backward facing steps and the transversely injected fuel jets. Penetration of a fuel jet into a supersonic airstream creates a shock upstream of the jet. The underexpanded sonic fuel jet itself undergoes further expansion resulting in barrel shocks and Mach disks. Also, recirculations usually occur upstream and downstream of the jet. The most difficult physical phenomenon to resolve computationally is probably the turbulent mixing of the transverse jets and the airstream. When the mixing is taken care of, then one has to be concerned with the kinetics of the combustion processes. A single computational study probably cannot address the whole array of the mentioned physical phenomena.

Experimental Study

The test hardware used in this study is shown schematically in Figs. 1–3. The injector region consisted of five small pilot fuel injector holes (0.050 in. diam), 10 injector diameters apart, located at an axial position 37 injector diameters upstream of a backward facing step of height h (=0.15 in.). These pilot injectors supply a small amount of fuel to the boundary layer approaching the step for flameholding purposes.

The ignitor fuel used in the test was a mixture of 20% (by volume) monosilane (SiH_4) and 80% hydrogen. Hereafter, the ignitor fuel will be referred to as silane. The silane jets were turned off after the flames from the primary jets stabilized.

The primary fuel injectors (0.120 in. diam) were located at a distance of approximately 12 step heights downstream of the step. This distance is downstream of the reattachment point of the mainflow, and hence the primary fuel should not feed upstream into the recirculation region behind the step. This prevents it from quenching the reaction by creating a cool, very fuel-rich zone. The purpose of the pilot-fuel/step combination is to provide a continuous ignition source for the primary fuel. The final combustor section consisted of a 48-in.-long diverging duct with an expansion half-angle of 2 deg. This is the region where most of the fuel mixed and burned.

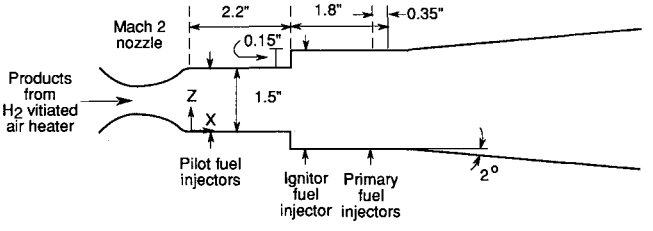

Fig. 1 The x-z plane schematic of the test apparatus.

Presented as Paper 88-3259 at the AIAA/SAE/ASME/ASEE 24th Joint Propulsion Conference, Boston, MA, July 11–13, 1988; received Nov. 4, 1988; revision received Oct. 13, 1989.

*Research Engineer; currently Senior Research Associate, Institute for Computational Mechanics in Propulsion, NASA Lewis Research Center.

†Research Scientist, Fluid Mechanics Division, Experimental Methods Branch.

Table 1 Inflow and jet conditions

	M	T, °R	P, atm	ϕ_1	ϕ_2
Case 1	2	1460	1	0.05	0.369
Case 2	2	2150	1	0.05	0.430

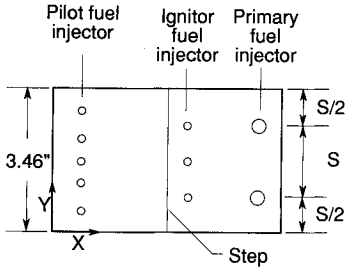

Fig. 2 The x-y plane schematic of fuel injectors region.

The high enthalpy test gas required to simulate scramjet combustor flow for flight Mach numbers ranging from 4 to 7 was produced by a hydrogen-air burner. Oxygen was then added to the combustion product such that its content was nominally 21% by volume, the same as air; this type of air has been referred to as vitiated air.

The inflow and the jet conditions of the two cases that were computed are summarized in Table 1.

Wall-surface pressures were measured at various points along the injector block and down the divergent duct. The experimental wall-pressure distribution will be used to compare with those obtained by the CFD prediction. Greater details of the experiment can be found in Ref. 1.

Computational Fluid Dynamics Study

Description of the Code

The CFD code SCAMM3D (supersonic combustion analysis using MacCormack method) used in this study was developed by Uenishi.[2] The code has been modified somewhat to make it more accurate, efficient, and readable. The code uses a finite-difference technique based on the MacCormack algorithm to solve nine partial differential equations that govern three-dimensional flow of the reacting hydrogen-air system. The governing equations consist of five fluid-dynamics equations in fully elliptic form and four species transport equations for total hydrogen, molecular hydrogen, water, and OH species. These four species are the result of the finite-rate, two-step combustion model[3] that was used in this study. The model can be written as

$$H_2 + O_2 \rightleftharpoons 2OH$$

$$2OH + H_2 \rightleftharpoons 2H_2O$$

The combustion model yields a stiff system of governing equations that necessitates an implicit treatment of the chemistry production terms in the species equations. The implicit source terms allow the governing equations to be integrated with a fluid time scale, which is much larger than the chemistry time scale, resulting in considerable savings in computer resources. The code is written in CDC Fortran 200, a vector language, and is operational on the Cyber 205 computer. Execution time was about 1.1×10^{-5} s per iteration per grid point.

Grid Generation

The number of grid points used was $91 \times 37 \times 30$. The origin of the computational coordinates was at the lower right corner of the inflow plane just downstream of the nozzle exit (see Figs. 1–3). Because the configuration is symmetrical, only the lower right quadrant of the configuration was solved (Fig. 3). Grids were generated by a simple algebraic function, which allowed specification of the size of the first (or last) grid and the rate of growth of subsequent grids. Clusterings of grid points were made near the fuel injectors, solid boundaries, and step. The pilot fuel injector was represented by just one grid point; the primary fuel injector was represented by 12 grid points. In the previous study,[2] the fuel jet was modeled by a square hole; this could alter the aerodynamic and mixing characteristic of the jet. In this study, an improvement was made by modeling the jet with an octagon, which had a diameter of 4 grids and the edges of 2 grids. This is the same as a 4×4 grid square jet with the four grids at the corners stripped off. The area of the octagon was set to be the same as the area of the round jet.

The computational domain began 2.2 in. upstream of the step and ended 4.5 in. downstream of the 2-deg expansion corner. The computation was done on a structured computational domain, which had uniform grids everywhere.

Boundary Conditions

At the inflow boundary, the flow was assumed to be uniform; necessary data were fixed to the values given in the previous section. In reality, the flow was not uniform because of the presence of the boundary layers. However, the boundary layers in this case were quite thin because the flow just exited from a short Mach 2 nozzle without an additional constant area duct in between. In future studies, boundary-layer effect will be included and evaluated.

Along the solid walls, no slip conditions ($u = v = w = 0$) were imposed together with the zero normal pressure gradient ($\partial p/\partial n = 0$), constant-temperature wall, and noncatalytic walls ($\partial f_i/\partial n = 0$).

On the top and the left boundaries, symmetry conditions were implemented. Flow quantities at the outflow boundary were obtained by extrapolation from the adjacent upstream station. Implicit in this procedure was the assumption that the flow at the exit was mainly supersonic. Conditions at the jet points were simply fixed at the experimental values.

Turbulence Models

In the previous study,[2] the Baldwin-Lomax turbulence model was used exclusively. This turbulence model,[4] however, has its basis on boundary-layer-type flows. The mixing length required in the model is based on the distance from a solid wall. Obviously the Baldwin-Lomax model alone is not applicable to the present problem where the main feature of the flowfield is the mixing of the transverse jets with the airstream. In this study, the jet-airstream mixing process was accounted for by a Prandtl mixing length model. The Baldwin-Lomax turbulence model was used only within the boundary layers close to solid walls.

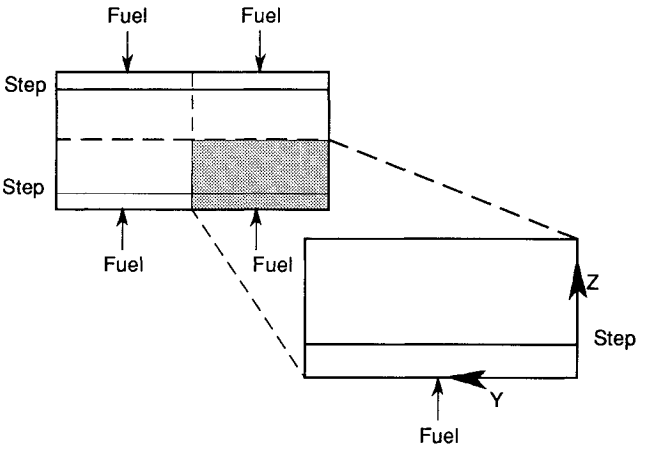

Fig. 3 The y-z (cross-sectional) plane schematic showing the quadrant of the computational domain.

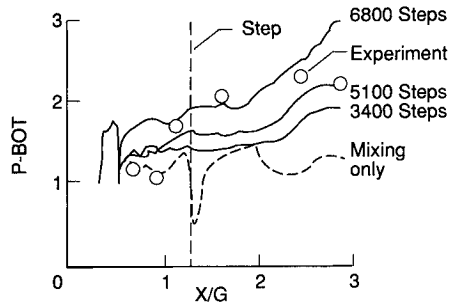

Fig. 4 Bottom wall surface pressures of case 1.

The greatest advantage of the Prandtl length model is its simplicity. The model can be written as

$$\mu_t = k\rho\omega l^2$$

In this study, k was set equal to 0.025; this value was obtained from a calibration with experimental data in a two-dimensional calculation.[5] The mixing length was calculated at each x plane, starting somewhat downstream of the primary jet in order to avoid the nonparallel flow in the vicinity of the jet exit. Traditionally, the mixing length is taken as the half-velocity width of the jet. In this study, however, velocity profile could be very oscillatory as the result of the presence of shock waves in the flowfield; use of a half-velocity width is, therefore, not a very expedient choice. It was conjectured that use of a half-concentration width would be more appropriate. At any x station, the center line (y=const) of the jet was located and searched for the maximum of the "total" hydrogen (i.e., hydrogen concentration in all forms). This maximum concentration point was defined as the center of the jet. From the center point, the search continued in the four directions (y^+, y^-, z^+, z^-) to find four half-concentration widths. A half-concentration width is defined as the distance from the jet at which its total hydrogen concentration is equal to half of that at the jet center. The mixing length was then taken as the arithmetic mean of the four half-widths. Use of total hydrogen rather than molecular hydrogen allows the computation of both combusting and noncombusting flows since in the combusting flow, molecular hydrogen could be totally consumed.

It is not an intention of this study to simulate turbulence-combustion interaction, although it is acknowledged that it could be important. Results obtained in a two-dimensional simulation of supersonic combustion in a coaxial jet burner,[5] however, seem to indicate that turbulence-combustion interaction is not important.

Solution Procedure

The computation was started with a uniform distribution of dependent variables everywhere except for that behind the step where a linear distribution was used. The integration time step and the jet pressures were ramped up gradually over 200 time steps to avoid a code failure because of abrupt disturbances.

The noncombusting case was solved first. Once a noncombusting solution was obtained, the chemistry was turned on. First, to simulate the silane ignitor behind the step, the ignition temperature was set to be 900°R, and the activation energies of the combustion model were reduced to half of those of the physical values. When a pocket of hot gas appeared behind the step, the ignition temperature was set to 1800°R, and the activation energies were reset to their physical values.

It is appropriate to mention here that the two-step kinetics used in this study cannot accurately predict autoignition. In the computer code, ignition is assumed if the temperature of the mixture is above 1800°R. The kinetic model, however, was designed mainly to predict total reaction time of the mixture, which is of major concern in engineering applications.

In initial runs, it was observed that too much fuel (higher than the experimental value) was injected into the airstream. This occurred because uniform profiles of fuel flow were assumed at the fuel jet exits. A remedy to this was to calculate the fuel mass flow rates that would give the experimental equivalence ratios. To achieve this, the pressures of the fuel jets were reduced while using the same jet cross-sectional areas. Alternatives would be to put in appropriate profiles at the jet exits (a very tedious task) or to reduce the injector areas to account for discharge coefficients. It is interesting to note that lower jet pressure produces the same jet penetration as the higher pressure case provided that the equivalence ratio is the same. So, lowering of the jet pressures should not alter the qualitative behavior of the jet.

Steady state of a solution was observed by monitoring of the maximum and average density residual, the physical time of the integration, and the fluctuations of pressures at selected mesh points in the flowfield. The flow of the present study probably will never achieve a steady state resulting from interactions of shock waves and recirculation zones; however, the fluctuations appeared to be bounded about mean values.

Results and Discussion

Two classes of problems, namely large scale and small scale, were studied in the experiment. In the present CFD study, only two cases of the small-scale combustor were investigated (see flow conditions in the previous section). Both cases had fairly low equivalence ratios and differed mainly in the total temperatures. The first case had a total temperature of 2400°R, and the second case had a total temperature of 3760°R, which correspond to flight Mach numbers of approximately 5 and 8, respectively. The Reynolds number based on step height of the two cases are 3.75 and 2.45×10^3, respectively. Calculations were made only within the near field of the fuel injectors, $X/G = 3$ for the first case and $X/G = 4.7$ for the second case.

Results of case 1 are shown in Figs. 4–7. The nonreacting flow, with fuel jets on, was solved first; then the chemistry was turned on and the iteration continued. Various normalized pressure distributions along the bottom wall of the x-z plane at $y = 1.73$ in. (i.e., the midplane) are plotted vs the x axis (normalized by the gap width) in Fig. 4. The local peaks of the pressure distributions near the inflow boundary are the pressure of the pilot fuel jet. It is clearly seen from the figure that, for the nonreacting case, the flow expanded over the step and finally recompressed back to the freestream value. For the reacting case, however, there was no reattachment point behind the step. This result indicates that the pressure

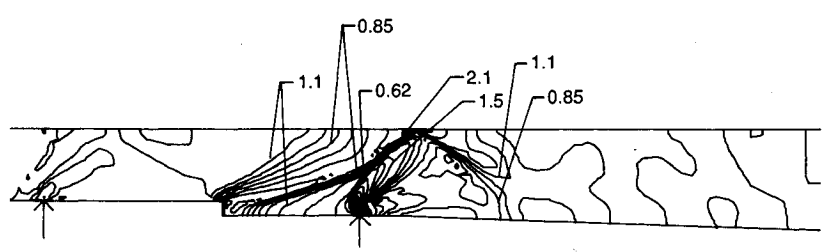

Fig. 5 Pressure contours on the x-z plane through the primary jet.

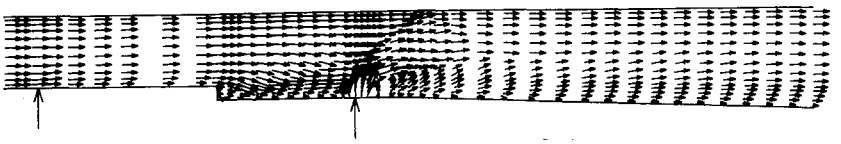

Fig. 6 Velocity vectors on the x-z plane through the primary jet.

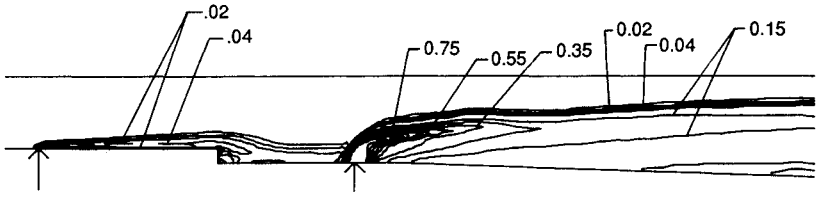

Fig. 7 Hydrogen concentration contours on the x-z plane through the primary jet.

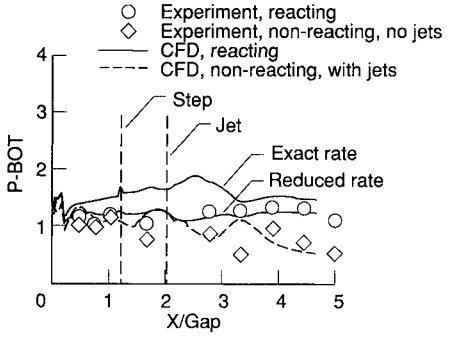

Fig. 8 Bottom wall surface pressures of case 2.

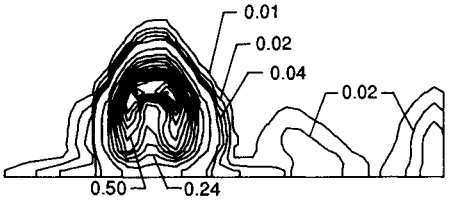

Fig. 9 Hydrogen concentration contours on y-z plane at $x = 5$ in.

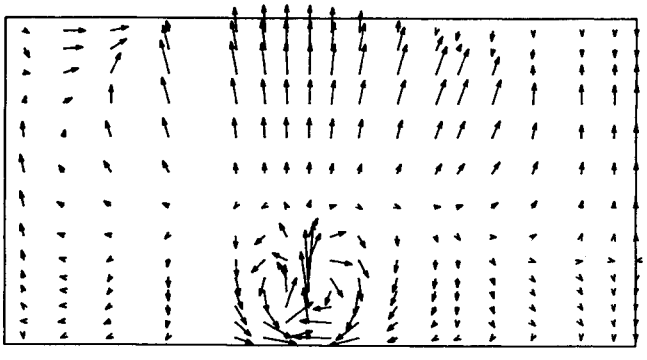

Fig. 10 Velocity vectors on y-z plane at $x = 5$ in.

behind the step was high due to heat release of the combustion. As can be seen in Fig. 4, the wall pressure increases continuously as the numbers of iteration increase. Beyond 6800 time steps, the flow thermally choked as indicated by a standing normal shock wave at the inflow boundary. The experimental results did not indicate a choked flow; however, a closer examination revealed that it was almost choked (identified in Ref. 2 as upstream interaction). It was argued initially that a slight numerical error caused the choking. Figures 5, 6, and 7 portray the pressure contours, the velocity vectors, and the hydrogen contours, respectively, of the plane through the primary jet for the nonreacting case. The expansion fan, the recompression shock wave, and the separation bubble behind the step are clearly seen. The recompression shock is finally merged with the jet bow shock. Two Mach disks are seen also near the exit of the primary jet. The jet shock reflects from the upper (symmetrical) boundary but does not reflect as much from the lower solid wall because of the weakening effect of the expansion of the flow following the 2-deg divergent nozzle.

To move the flow regime further away from the choke point, the second case was solved. This case has a higher enthalpy than case 1. The length of the computational domain was also extended to 8.5 in. ($X/G = 4.7$). Figure 8 shows the pressure distribution along the bottom wall as compared to that of the experiment. The plot indicates that the computation, with exact kinetics, considerably overpredicted the surface pressure. This overprediction was believed to be caused by too fast a reaction rate. The choking of the first case was probably caused by the fast chemistry as well, but it was not recomputed because of time limitation.

The combustion model used in this study[3] has pre-exponential coefficients, which are functions of the equivalence ratio (ϕ). The allowable range of ϕ is from 0.2 to 2.0, and the higher the ϕ the lower the combustion rate. To study the effect of kinetics, case 2 was rerun with the rate coefficients set equal to those at $\phi = 2$ throughout the flow. The results of this case are shown in Fig. 8 together with the results of the nonreacting flow and experimental data points. Note that the nonreacting flow was computed with the fuel jets on which is not exactly the case of the experiment; nevertheless, the pressure distributions follow the same trend. The distribution of the reacting case is now in quite good agreement with that of the experiment. Further study is definitely in order to settle this kinetics-dependent issue. Also evident from the results of the high enthalpy case is that there is no reattachment point (even for the nonreacting case). The separation bubble over the step completely merged with the separation bubble induced by the primary jet.

Although not shown, mixing and combustion efficiencies were computed. The CFD results underpredicted the mixing efficiency (computed from a generic mixing correlation) and the combustion efficiency (computed from global pressure rise) by about 20%. It should be noted that the calculations lumped the vitiated water with the nitrogen species to form a new pseudonitrogen gas. Had this lumping not been done, the ϕ would have been somewhat higher than that used in the present calculation. In the future study, the effect of not lumping water with nitrogen will be investigated. The mixing efficiency can be increased by adjusting the k value of the mixing model, but this was not done in the present study.

Finally, the cross-sectional (y-z) plots at $x = 5$ in. are shown in Figs. 9 and 10. The characteristic kidney-shape cross section of the hydrogen contours is evident in Fig. 9. Figure 10 further reveals the two counter-rotating vortices, which is an important physical phenomenon associated with a jet injected into a crossflow.

Conclusion

The reacting flowfield inside a generic, small-scale scramjet combustor has been obtained using a three-dimensional fully elliptic computer code. The hydrogen-air combustion was simulated by a four-species, two-step, finite-rate combustion model. It was found that an adjustment to the equivalence-ratio-dependent, pre-exponential coefficients in the combustion model was necessary in order for the CFD results to agree well with the experimentally measured wall pressures. Many qualitative aerodynamic features of the flowfield such as flow turning over the step, jet shock, Mach disks, and counter-rotating vortices were well predicted by the CFD code. The simple Prandtl mixing length scheme that was used to simulate the mixing of the jet in the supersonic crossflow seems to perform well. The computer code needs to be further validated with relevant experimental data before it can be used on a routine basis for design purposes.

Acknowledgments

Research support for the first author was by NASA under NASA Contract NAS1-17919. The authors would like to acknowledge Glen S. Diskin for providing the experimental data. Useful discussions with R. Clayton Rogers are also appreciated.

References

[1]Diskin, G. S., and Northam, G. B., "Effects of Scale on Supersonic Combustor Performance," AIAA Paper 87-2164, June 1987.

[2]Uenishi, K., Rogers, R. C., and Northam, G. B., "Three-Dimensional Computations of Transverse Hydrogen Jet Combustion in a Supersonic Airstream," AIAA Paper 87-0089, Jan. 1987.

[3]Rogers, R. C., and Chinitz, W., "Using a Global Hydrogen-Air Combustion Model in Turbulent Reacting Flow Calculation," *AIAA Journal*, Vol. 21, No. 4, 1983, pp. 586–592.

[4]Baldwin, B. S., and Lomax, H., "Thin Layer Approximation and Algebraic Model for Separated Turbulent Flow," AIAA Paper 78-257, Jan. 1978.

[5]Jarrett, O., Jr., Antcliff, R. R., Cutler, A. D., Chitsomboon, T., Dancey, C. L., and Wang, J. A., "Measurements of Temperature, Density, and Velocity in Supersonic Reacting Flow for CFD Code Validation," *Proceedings of the 25th JANNAF Combustion Meeting*, Vol. 1, Chemical Propulsion Information Agency, Laurel, MD, CPIA Pub. 498, Oct. 1988, pp. 357–364.